Scientific African 25 (2024) e02262

Contents lists available at ScienceDirect

Scientific African

journal homepage: www.elsevier.com/locate/sciaf

Spatio-temporal land use and land cover change assessment: Insights from the Ouémé River Basin

Ernestina Annan [a,*], William Amponsah [b], Kwaku Amaning Adjei [c], Markus Disse [d], Jean Hounkpè [e], Ernest Biney [a], Albert Elikplim Agbenorhevi [e], Wilson Agyei Agyare [b]

[a] WASCAL Climate Change and Land Use, College of Engineering, KNUST, Ghana
[b] Department of Agricultural and Biosystems Engineering, College of Engineering, KNUST, Kumasi, Ghana
[c] Department of Civil Engineering, College of Engineering, KNUST, Kumasi, Ghana
[d] Chair of Hydrology and River Basin Managment, Technische Universität München (TUM), Munich, Germany
[e] WASCAL Climate Change and Water Resources, Institut National de l'Eau, Université d'Abomey-Calavi, Cotonou, Benin

ARTICLE INFO

Editor: DR B Gyampoh

Keywords:
Accuracy assessment
Google earth engine
Supervised classification
Image composition
Landsat
Tropical basin

ABSTRACT

The rapid increase in population and urban development are exacerbating the transformation of natural environments into unnatural forms. While detailed assessment of the environment is beneficial for efficient ecosystem system management, it can also be time and resources-consuming. This study aimed to map and quantify the spatio-temporal changes in land use and land cover (LULC) using the Ouémé River Basin as a case study. The supervised classification in Google Earth Engine (GEE) cloud-computing platform was employed to distinguish Landsat images for 1986, 2000, 2015 and 2023 into forest areas, settlements/bare lands, savanna areas (woodlands), agricultural lands and water bodies. Analysis of the LULC changes revealed that savanna areas and woodlands which were predominant in the basin in 1986 have steadily declined by 24 % in area in 2023. Forest areas have diminished by 4.3 % at an annual rate of 4 %. Agricultural lands have however grown exponentially by 28 % since 1986, with a more rapid increase between 2015 and 2023 at an annual rate of 3.7 %, driven by rising food demand due to population growth within and around the basin. Settlements and bare areas tripled in area, reflecting a similar trend to Benin's urban population growth. Accuracy statistics of the LULC classification showed overall accuracy and kappa statistic values above 90 % and 86 %, respectively, indicating the admirable performance and reliability of the Simple Composite Landsat algorithm for image composition, and the Random Forest Classifier for LULC classification approach applied in this study. The approach also demonstrates the robustness and potential of LULC mapping in large and complex ecosystems using the GEE cloud-based remote sensing tool, which is underutilized in the study area. Overall, the LULC trends provide beneficial insights useful to policy-makers and any other stakeholders involved in sustainable ecosystem management planning in the basin.

* Corresponding author at: Department of Civil Engineering (WASCAL), College of Engineering, KNUST, Kumasi, Ghana.
E-mail address: ernestinaannan39@gmail.com (E. Annan).

https://doi.org/10.1016/j.sciaf.2024.e02262
Received 24 November 2023; Received in revised form 16 May 2024; Accepted 27 May 2024
Available online 27 May 2024

Introduction

The rapid population growth and urban development are increasing the demand for water and food [1]. These factors have led to significant increase in the conversion of naturally vegetated areas into croplands to meet the growing population food supply, impacting overall ecosystem health. Land use and land cover (LULC) changes contribute to altering precipitation and temperature patterns within regions [2–4]. These changes affect the ability of ecosystems to provide essential services including food and water. Agriculture is crucial to West Africa's economic growth, employing more than 60 % of the workforce and contributing 26.9 % to Benin's GDP [5]. However, freshwater availability is limited spatially and temporally, impacting its use for domestic, agricultural and industrial purposes [6].

Approximately 80 % of Benin's population, totaling over 13 million people, rely on agriculture, primarily subsistence farming under rain-fed conditions. In 2014, more than 60 % of the population were reported to have had access to potable water [7]. The same report of the institute added that there is limited information on the differences in accessibility or availability of water resources in the landscape. Ecosystem processes, such as carbon and hydrological cycles and climate change, are complex to understand and predict. Nevertheless, continuous monitoring provides valuable insights for sustainable management. For instance, it can support efforts to improve the implementation of integrated water resources management to achieve SDG Target 6.5 (by 2030, implement integrated water resources management at all levels, including through transboundary cooperation as appropriate) which lags globally [8].

Mapping changes in LULC plays a vital role in assessing environmental transformations. It helps identify shifts in vegetation types and provides insight into spatio-temporal changes in regional hydrology [9]. Such mapping is crucial for achieving SDG target 15.1, which aims to ensure the conservation, restoration and sustainable use of terrestrial and inland freshwater ecosystems and their services, including forests, wetlands, mountains and drylands by 2020, in line with obligations under international agreements.

Today, the inaccessibility of certain areas of interest and the need for rapid results to inform decision-making have prompted the utilization of Geographic Information Systems (GIS) and Remote Sensing applications. These complement field measurements by providing additional environmental data. When combined with modeling tools, they enhance the visualization, manipulation and interpretation of data across different spatial and temporal scales. Cloud-based remote sensing platforms, such as the Google Earth Engine (GEE), facilitate the analysis of large data sets and extensive geographical areas efficiently. GEE hosts a diverse range of satellite datasets at various resolutions, facilitating studies on environmental change.

Images obtained from remotely sensed sources, such as satellites, over time, offer valuable insight into changes in LULC [10]. This information can be used to assess the impact of LULC on ecosystem processes and its ability to provide essential services.

The Ouémé region has been extensively studied for its environmental changes, with international initiatives such as IMPETUS (An Integrate Approach to the Efficient Management of Scarce Water Resources in West Africa) and the RIVERTWIN projects contributing significant insights. Through the IMPETUS project, Hiepe [11] utilized the Soil and Water Assessment Tool (SWAT) with Landsat imagery to model soil degradation in the upper Ouémé River Basin. Results revealed that the north-western, eastern, and north-eastern areas are soil erosion hotspots due to rapid agricultural expansion driven by high population growth.

The RIVERTWIN project produced the 2003 land cover map of the Ouémé River Basin which has been instrumental in LULC change studies across various subbasins [12,13]. Bodjrènou et al. [14] evaluated LULC change in the basin using the US Geological Survey (USGS) West African Land Cover Times Series for 1975, 2000 and 2013, revealing a trend of agricultural intensification.

Osseni et al. [9] assessed the changes in vegetation cover in the Ouémé Delta, south of the Ouémé River Bonou outlet, noting extensive fragmentation and replacement of natural vegetation by agricultural lands and road networks due to population growth and urbanization. Additionally, according to Hounkpè et al. [15], municipalities within the Ouémé River Basin face increasing vulnerability to climate change unless adequate adaptive measures are implemented.

These studies, alongside initiatives like the Food and Agriculture Organization (FAO) Ouémé River Basin Climate-Resilience Initiative (OCRI) Benin for improved food productivity, underscore the Ouémé River Basin's critical role in the country's food security and ecosystem sustainability. However, increased anthropogenic influences disrupt the environment's natural replenishment processes, leading to heightened risks of droughts and floods. Mapping changes LULC becomes challenging due to the large spatial size of images, especially fine resolution ones. They often require lengthy download and processing times and occupy significant storage space, particularly when working with extensive areas. The GEE cloud-based remote sensing tool offers an interactive platform for accessing diverse satellite data and conducting LULC classification, accuracy assessments and change detection. It enables secure storage of data and projects, with easy access to previous projects through retrieval links. This is particularly beneficial for the Ouémé River basin which lacks sufficient information on historical LULC dynamics, a gap this study aims to fill.

While other tools have been used to assess LULC change in the area, further research is needed to explore robust technologies like cloud computing technology and machine learning, which remain underutilized. The study delves into utilization of the Simple Composite Landsat algorithm for compositing time series Landsat images within Google Earth Engine. Although this approach is relatively uncommon in LULC classification assessments, it holds promise for advancing remote sensing methodologies. Streamlining the management and analysis of environmental datasets is crucial for achieving sustainable use of terrestrial ecosystems and their services, as by SDG target 15.1.

Therefore, this study aims to evaluate LULC change within the Ouémé River Basin leveraging GIS and cloud-based remote sensing tools. The specific objectives include (i) mapping spatio-temporal changes in LULC types, (ii) assessing classification accuracy, and (iii) quantifying the extent and rate of LULC change. The study utilizes the Simple Composite Landsat algorithm for image composition and the Random Forest Classifier within Google Earth Engine, a machine learning tool for supervised classification of LULC. The findings will provide valuable insights into environmental dynamics in the Ouémé River Basin, aiding stakeholders in making informed decisions for sustainable management decisions.

Study area and data sources

The Ouémé River Basin

The study area is the Ouémé River basin (Bonou), which is located between latitudes 6° 30′ N and 10° 00′ N, and longitudes 0° 52′ E and 3° 05′ E. Its surface area is about 50,000 km^2 with 89 % in Benin, and 10 % and 1 % in Nigeria and Togo respectively. It covers about 43 % of Benin [14], which makes the basin an important land resource for both water and agriculture in the country. The Ouémé River Basin lies in the transition between the northern and southern parts of Benin and has three different zones according to the differences in weather variables such as rainfall and temperature.

The northern part of the basin has a unimodal rainfall regime with single rainy and dry seasons, while the southern part has bimodal rainfall regime with two rainy and dry seasons where the dry season is shorter than the northern part. The average rainfall of the basin is about 1050 mm, and temperature values range from 25 °C to 30 °C [1]. It is bounded above by the Atakora Mountains, and forms a large Delta in the South at Cotonou, and discharges into the Gulf of Guinea at an average rate of 170 m^3/s. According to the Koppen climate classification, the Ouémé River Basin falls in the Tropical Savanna climate zone [16]. Its largest tributaries are the Okpara River on the left and the Zou River on the right sides (Fig. 1). The soil of the region is mainly ferralitic, highly weathered, rich in sesquioxide and mostly kaolinitic, with some changes in texture within the soil profile [17].

Data sources

Land use and land cover data were obtained based on considerations of data quality, accessibility, and the need for substantive information on LULC changes. Four Landsat Tier 1 scenes of land use/cover for the entire basin were acquired for the dry season in the years 1986, 2000, 2015 and 2023 (Table 1). All images were selected from 1st January and 31th March, and extended to 30th April where image quality was insufficient. Images captured during the dry season exhibit lower percentages of cloud cover compared during the rainy season. A high percentage of clouds in an image obscures the level of detail needed to achieve high accuracy values in classification. Therefore, images with lower cloud cover are recommended to improve classification accuracy in GEE.

The GEE cloud computing database facilitates faster analyses through cloud processing and integrates various datasets at varying resolutions, which are updated and expanded daily. For large basins like the Ouémé River Basin, GEE provides a fast and straightforward means of assessing land use and cover changes that have occurred within the basin for the past 38 years [18].

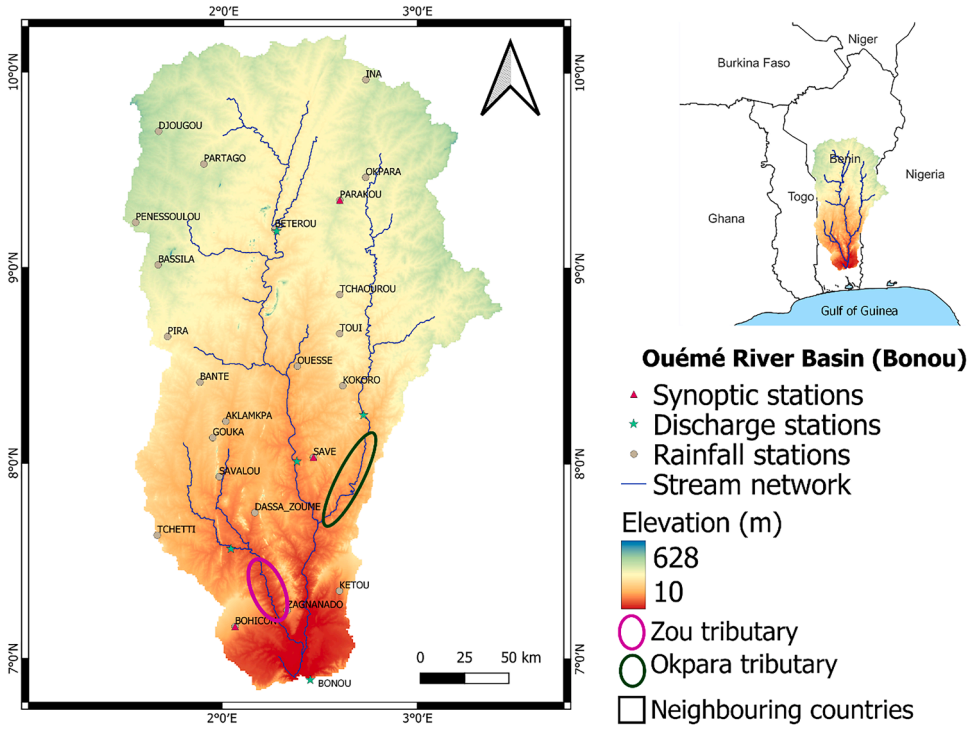

Fig. 1. Elevation Map of the Ouémé River Basin (m) showing locations of rainfall and discharge measuring stations.

Table 1
Satellite data used for LULC classification.

Year	LULC data used	Resolution	Number of images available
1986	Landsat 5 TM	30 m	27
2000	Landsat 7 ETM+	30 m	23
2015	Landsat 8 OLI/TIRS	30 m	55
2023	Landsat 8 OLI/TIRS	30 m	57

Methods

Data composition

Image composition is a crucial aspect of assessing time series LULC data. In this study, we employed the 'Simple-Composite Landsat algorithm' available in the GEE interface (https://developers.google.com/earth-engine/guides/landsat). This algorithm utilizes radiometrically and geometrically processed Tier 1 scenes of the images by selecting a subset from each location and converting them to Top of Atmosphere (TOA) reflectance. It selects the lowest possible range of cloud and shadow scores at each point and, using the Simple Landsat Cloud Score algorithm, calculates the median of the least cloudy pixels [19]. TOA reflectance for Landsat 5 TM /7 ETM+ and Landsat 8 OLI/TIRS is calculated using Eq. (1) [20] and Eq. (2) [21] respectively. This correction accounts for atmospheric effects, and differences in solar zenith angles and Earth-sun distance between different data acquisition dates and sensors.

This innovative algorithm in GEE for compositing Landsat images preserves spectral and spatial fidelity, and is crucial in LULC change detection, particularly challenging when using surface reflectance (SR) images due to data gaps created during cloud-masking. While this algorithm has been understudied, it has proven to enhance effective compositing of Landsat images and yield high mapping accuracy values [22,23].

$$\rho_\lambda = \frac{\pi L_\lambda d^2}{ESUN_\lambda \cos\theta_s} \tag{1}$$

$$\rho_\lambda = \frac{M_\rho Q_{cal} + A_\rho}{\sin(\theta_s)} \tag{2}$$

where;

ρ_λ = Planetary TOA reflectance [unitless]
π = Mathematical constant equal to approximately 3.14159 [unitless]
L_λ = Spectral radiance at the sensor's aperture $\left[W/(m^2\ sr\ \mu m)\right]$
$ESUN_\lambda$ = Mean exoatmospheric solar irradiance $\left[W/(m^2\ \mu m)\right]$
θ_s = Solar zenith angle [degrees]
M_ρ = Band-specific multiplicative rescaling factor from the metadata
Q_{cal} = Quantized and calibrated standard product pixel values (DN)
A_ρ = Band-specifc additive rescaling factor from the metadata

Therefore, the code for input in GEE for image composition requires;

- Image Collection to be used (e.g., Landsat 5 TM Tier 1 scenes)
- Region of interest (roi) which is a shapefile of the study area
- period of interest (e.g., 1986-01-01 to 1986-03-31)
- select input bands of interest

LULC classification

Stratified random sampling technique was employed to select training samples by polygons, where random sampling was independently performed for each land-cover type according to the proportion of the Landsat image covered by the type, as recommended for land use classification [24]. These training samples were collected from Google Earth Pro, field visit and GEE base maps, following the good practices for assessing land use change outlined by Olofsson et al. [24]. Ground-truth points and polygons were initially collected for the current year, 2023, through field visits to the study area and the high-resolution satellite layer of Google Maps using Google Earth Pro interface. The 'historical imagery' tool in Google Earth Pro allowed visualization of Google Maps from historical years, aiding collecting reference data for 1986, 2000 and 2015. To collect training data, the reference data was imported into GEE and superimposed as a shapefile on the Landsat composite images. The training data was generated based on the LULC types using the spectral indices and visual interpretation of the land features.

A total of 1471 training/validation polygons were randomly generated throughout the basin in GEE for the four years, with 70 %

allocated for training and 30 % for testing of the classification method. Polygons were used instead of points to enable uniform collection of more pixel information on LULC types considering the large size of the basin. The variable 'count' was applied to the algorithm to determine the number of images sampled for compositing in each year (refer to Table 1S in the supplementary material). To ensure higher accuracy of classification of features in the raster images, auxiliary variables including the Normalized Difference Vegetation Index and Bare Soil Index were computed for the composite images of each time step and added to the image band set [19, 25].

Five LULC classes were considered for the study, based on the FAO West African LAND Cover Reference System [26], as described in Table 2. A supervised classification was performed using the Random Forest classification algorithm embedded in GEE to group the land features of each of the Landsat composited images into the five different LULC classes. The ecosystem within the Ouémé River Basin consists mostly of a mixture of LULC types per area, where settlement areas are interspersed with farmlands, trees, plantations, and business centers, making it complex to map. One advantage of the Random Forest Classifier is its ability to handle high-dimension data with complex interactions between variables, although it is sensitive to errors in the input data [27]. Moreover, it has been proven to yield higher accuracy in land cover mapping and projections in Africa and many other parts of the world [23]. Furthermore, handling a large area like the Ouémé River Basin is robust in GEE, and provides a wide variety of satellite data and faster data visualization and analysis. The classification step therefore requires;

- a composited image
- feature collection containing training/validation polygons collected for each LULC class and given the same property name and specify percentage for training and validation.
- the output bands of interest (e.g., Landsat 5 bands, NDVI, BSI)
- extract confusion matrices of the training and validation
- Output folder to export classified map (e.g., google drive).

Accuracy assessment

The cross-tabulation matrix (error matrix) of the validation sample in pixels extracted from GEE was utilized for the accuracy assessment computations. The accuracy of the LULC classification for the four maps was evaluated using summary statistics such as the overall accuracy (OA), producer accuracy (PA), user accuracy (UA), and kappa statistic. Values of overall accuracy and kappa statistic above 85 % and 80 % respectively, are considered indicative of strong to almost perfect agreement between the reference and predicted classification categories [28]. Additionally, area-based statistics, recommended to address uncertainties and biases in the classification process, were conducted. Accuracy was determined at the category scale (per each LULC class) and for the overall classified image. The confusion matrix was converted into an area-based matrix representing the entire study area to compute unbiased area-based summary statistics of the classified image using Card's equations [24,29]. This method involves calculating the area proportion of the predicted map (ratio of area of a category to total area of basin), based on which the area-based summary statistics are recalculated. These statistics include the percentages of omission and commission errors quantified by the user and producer accuracies, respectively, standard error of area estimates, and corrected area estimates with 95 % confidence to account for uncertainty.

This approach, recommended in recent times in addition to the kappa value, enables assessment of classified maps based on the area proportions of the categories reduces biases that could arise from the sampling method [24]. Two indices were used to express the sum of omission and commission errors, namely, quantity disagreement and allocation disagreement. Quantity disagreement represents the difference between the classified map and validation data due to imperfections in the proportions of the categories, calculated as the difference between omission and commission errors (sum of proportion of the category in the classified map minus sum of proportion of the category in the reference from the error matrix). Allocation disagreement is the differences arising from mismatches in the spatial locations of the categories, expressed as the sum of exchange (pairwise) and shift (non-pairwise) confusion between categories [10,29].

Change detection

The Land Cover Change post-classification tool within the Semi-Automatic Classification plugin (SCP) in the QGIS interface was utilized to analyze LULC change between the classified images. This process generates a change map (Fig. 3) illustrating the differences in LULC between two maps and produces a change matrix indicating the persistence or transformation of LULC classes into other

Table 2
Description of land use/cover classes in the Ouémé River Basin.

LULC Type	Description
Forest areas	Areas with dense trees (including riparian forests) mostly classified forests
Settlements/Bare lands	Cities, roads, bare (cleared) areas, towns
Savanna areas (Woodlands)	Areas with sparse trees interspersed with grass, shrubs, bushes
Agricultural lands	Croplands, plantations, fallow lands
Water bodies	Rivers, lakes, wetlands and areas covered with water for all or most part of the year.

classes. The magnitude of change between years (absolute change), relative change (%) and annual rate of change (%) were then computed from the change matrix (refer supplementary material for details) using the equations below ([28]). Maps were created using ArcGIS and QGIS software.

$$\text{Absolute change, } AC = A_2 - A_1 \left(\text{km}^2\right) \tag{3}$$

$$\text{Relative Change, } RC = \frac{A_2 - A_1}{A_1} \ (\%) \tag{4}$$

$$\text{Rate of Change, } q = \left(\frac{A_2}{A_1}\right)^{\frac{1}{t_2 - t_1}} - 1 (\%/\text{y}) \tag{5}$$

where A_2, A_1 are areas of LULC classes at final and initial years, and t_2, t_1 are their respective years.

Results

Spatio-temporal changes in LULC types

The results of the LULC Change assessment of the four classified maps revealed that the Ouémé River Basin was originally covered with savanna areas and woodlands in its major parts (Fig. 2). These land units occupied more than 70 % of the total area of the basin in 1986, followed by agricultural lands and then forest areas (refer to Table 2S in the supplementary material for further detail). Settlement areas and water bodies had the least cover in the basin. In 2023, agricultural lands dominated the basin by covering about 51 % of the total basin area, followed by savanna areas, settlement areas and bare lands, forest areas and then water bodies. This indicates a considerable decline in savanna and forest areas, in contrast to an expansion in agricultural lands and settlement areas.

The period between 2015 and 2023 exhibited the highest and fastest rates of losses and gains in LULC, spanning fewer years compared to the periods 1986–2000 and 2000–2015. Specifically, savanna and forest areas showed sharp reductions in area at rates 3.0 %/y and 6.6 %/y, respectively, while agricultural lands and settlement areas and bare lands exhibited sharp increases at rates of 3.8 %/y and 3.7 %/y respectively. However, during the periods 1986–2000 and 2000–2015, the results revealed gradual annual changes,

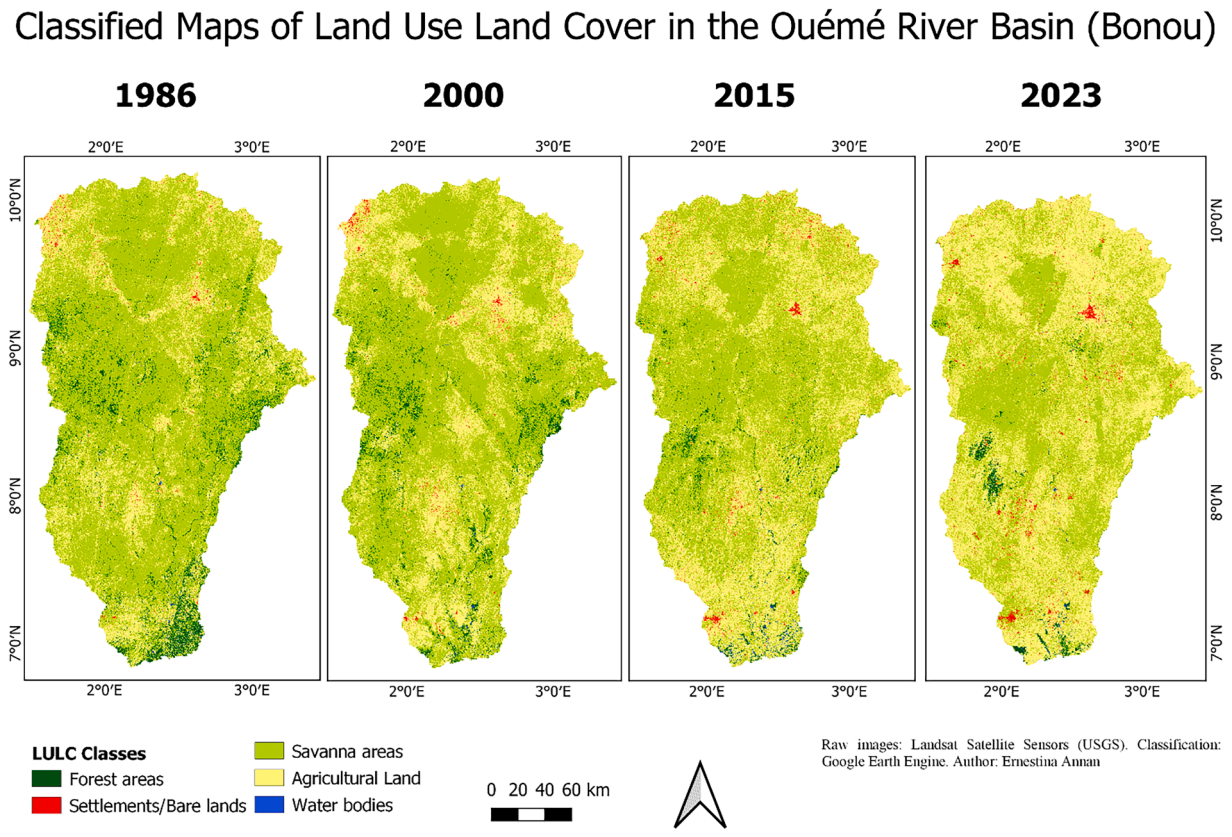

Fig. 2. Classified Maps of the Ouémé River Basin. It shows increasing agricultural land area and diminishing savanna and forest areas.

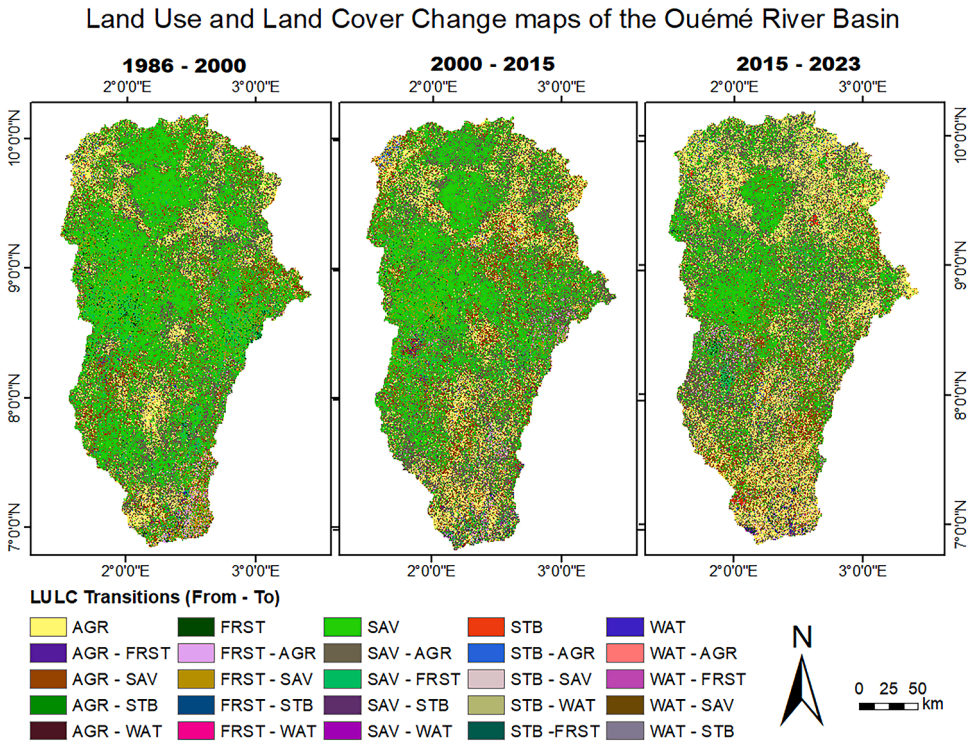

Fig. 3. Change Map of LULC in the Ouémé River Basin. It shows growing area of agricultural lands and diminishing savanna and forest areas. FRST, Forest areas; STB, Settlements/bare lands; SAV, Savanna areas; AGR, Agricultural lands; WAT, Water bodies.

with reductions in savanna areas (0.4 % and 0.8 %) and forest areas (1.9 % and 4.3 %) and increase in agricultural lands (1.5 % and 1.8 %).

Accuracy assessment

The supervised classification of LULC in the Ouémé River Basin for the year 1986, 2000, 2015 and 2023 yielded pixel-based accuracy values exceeding 90 %. Additionally, both producer and user accuracy values were also greater than 88 % and 85 %, respectively, for all four classified maps. Moreover, the kappa statistic values obtained were also above 85 % for all the maps (Table 3), indicating the reliability of the LULC maps for further analysis of changes in the basin.

The area-based accuracy analysis for the 2023 classified map yielded an overall accuracy value of 91.8 % ± 0.4, with commission (overestimation) and omission (underestimation) errors totaling 8.2 %. The quantity and allocation disagreement values were 2.3 % and 5.9 % respectively. Notably, the commission errors in agricultural lands estimation were of the equal magnitude to the omission errors in savanna areas estimation, while the omission errors in agricultural lands equaled to the commission errors in savanna areas. Additionally, the results indicated a 1 % underestimation in settlements areas and bare lands.

Overall, most of the errors stemmed misclassifications between savanna areas and agricultural lands, although a few forest areas were misclassified as savanna areas. Furthermore, some pixels of water bodies were misclassified as forest and savanna areas, particularly along riparian forests and swamps. The area of water bodies was higher in the 2015 classified map compared to the range of values observed in the other years, indicating an overestimation.

Conversely, the 1986 classified map, based on the area proportion analysis, demonstrated an overall accuracy value of 93.7 % ± 0.6, and a total error of 6.3 %. More than 50 % of the error were exchange and shift (allocation disagreement) errors, amounting to 3.3 % and 0.8 % respectively. Quantity disagreement summed to 2.2 %.

Table 3
Accuracy statistic of the LULC classification for each year based on their pixel and area-based error matrices.

Statistic	1986	2000	2015	2023
Pixel-based				
Overall accuracy (%)	92.90	92.58	90.63	92.93
Kappa statistic	0.90	0.89	0.86	0.90
Area-based				
Overall accuracy (%)	93.65	93.54	90.61	91.82

Regarding omission, savanna areas estimation had the highest omission errors of about 3 % followed by agricultural lands, settlement areas and bare lands, forest areas and water bodies having the least omission errors. This suggests that there were areas that should have been classified as the aforementioned LULC types but were either left out or misclassified as other LULC types. The value of exchange errors for savanna areas was the same as that for agricultural lands, indicating that most of the errors originated from misclassification between those two LULC types. Additionally, settlement areas and bare lands were largely underestimated, leading to a producer accuracy value less than 50 %.

Similar results were obtained for the year 2000 classified map, which had overall accuracy value of 93.5 % ± 0.5, and producer accuracy values ≥70 % for most classes, except for settlement areas and bare lands which had a value of 37 %. Furthermore, the area-based accuracy for the 2015 map yielded an overall accuracy of 90.6 % ± 0.5, with producer and user accuracy values ≥59 % and ≥87 % respectively.

The raw error matrix for the 2023 classified map, together with the producer, user accuracies (PA, UA), overall accuracy (OA) and area proportions of each LULC class values are provided in the supplementary material Table 3S. The corresponding area-based unbiased error matrix consisting the area proportions of each LULC class and the producer, user and overall accuracies and adjusted areas at 95 % confidence interval are also presented as supplementary material Table 4S.

Change detection of LULC types

The magnitude of forest cover loss exhibited a declining pattern over the period, yet the annual rate of deforestation increased, particularly during the period 1986–2000 compared to 2000–2015 (refer to Fig. 1S in the supplementary material). Approximately 78 % of the forest areas in the year 1986 have undergone degradation, resulting in a reduction of 2431 km^2 in area and an average 64 km^2 loss per year. Similarly, by the year 2023, savanna areas experienced a decline of approximately 11,867 km^2, representing a total loss of about 35 % of its cover in 1986, with an average annual loss of 312 km^2.

Conversely, agricultural lands multiplied by more than 100 % of their quantity in 1986, primarily as crop lands (maize, beans, cassava, yam, pepper and other vegetables) and plantations (cashew, oil palm, cotton, orange, tick), with an annual increase of 363 km^2. Settlements and bare lands also expanded by over 100 % of their area in 1986, resulting in a total gain of 534 km^2, with an annual increase of 14 km^2 per year expansion primarily in settlement areas. The rates of expansion during the period 2000–2015 were steeper than during 1986–2000 for settlements and bare lands, attributable to increasing population growth and urbanization rates.

Overall, the average annual rates of change between the years 1986 and 2023 were as follows: forest areas > settlements/bare lands > agricultural lands > savanna areas > water bodies, corresponding to −4.0 %, 3.0 %, 2.2 %, −1.1 % and −0.9 % respectively.

In summary, it can be inferred that savanna and forest areas have been actively converted into agricultural lands and settlements areas. Notable areas witnessing massive settlements expansion include Parakou and Djougou in the north, Bohicon and Ketou in the south, and Save and Dassa-Zoume in the central parts of the basin. Agricultural lands expansion, on the other hand, occurred throughout the basin, particularly in the north and southeast and west, encroaching into the savanna areas/woodlands, protected areas, 'classified forest' areas and along water bodies.

Discussion

The results reveal significant transformation in the Ouémé River Basin, with savanna areas being the predominant cover type in 1986. However, over time, large portions of these naturally vegetated areas have disappeared or been converted for other uses such as agricultural lands and settlements. This trend mirrors findings from previous studies by Bodjrènou et al. [14] and Osseni et al. [9], which also highlighted a decline in savanna areas and an expansion of agricultural lands. Additionally, assessments in neighbouring areas like the Couffo catchment further illustrate similar trends, emphasizing the widespread conversion of naturally vegetated areas into farmlands and settlement areas [30].

These transformations carry significant implications, including heightened erosion conditions and increased vulnerability to floods, as indicated by previous studies. Hiepe [11] identified erosion hotspots in the basin, particularly in areas experiencing rapid expansion of agricultural lands. Similarly, Bossa [13] found that soil degradation and sediment yield were sensitive to LULC changes in the basin, underscoring the environmental repercussions of such transformations. Furthermore, assessments by Hounkpè et al. [15] highlighted the vulnerability of Municipalities within the basin to climate events like flooding, particularly in areas where agricultural lands have expanded and natural vegetation has been lost. They include Djougou and Pèrèrè, and Bohicon, Covè, Glazoue, Zangnanado, Toffo and Djidja Municipalities.

The accuracy assessment of the classified maps demonstrated high agreement with the reference areas, indicating the reliability of the Simple Composite Landsat and the Random Forest Classifier algorithms with remotely sensed data in the GEE cloud computing platform for evaluating LULC information. However, challenges remain, particularly in accurately classifying settlement areas and bare lands, which exhibit similarities in appearance and reflectance with agricultural lands and savanna areas, especially during the dry season considered in this study. The presence of clouds and the resolution of the Landsat image also influenced classification accuracy, highlighting the need for further refinement in classification methods and the potential benefits of higher-resolution satellite data [31,32].

Overall, the findings underscore the importance of monitoring and understanding LULC changes in the Ouémé River Basin to inform sustainable land management practices and mitigate environmental risks associated with ongoing transformations.

The most significant transformations in the Ouémé River Basin have involved the conversion of forest and savanna areas into

agricultural lands and settlement areas. These changes have accelerated in recent years, particularly between 2015 and 2023, reflecting trends observed in previous studies by Bodjrènou et al. [14] and Osseni et al. [9], These findings align with assessments of land use change in Benin by the USGS, which identified the country as experiencing high rates of annual agricultural land expansion.

The rapid loss of tree cover in the basin has negatively implications for ecosystem functioning, as forests and savannas serve as crucial carbon sinks. Consequently, the degradation of natural vegetation contributes to increased carbon emissions and exacerbates global warming and climate change [33]. Moreover, the susceptibility of the basin to extreme events like flooding is exacerbated by the degradation of natural vegetation, as highlighted by studies assessing flood risks in the region [34,35].

Population growth within and around the basin emerges as a primary driver of anthropogenically-influenced land use and land cover change. Increasing population leads to greater demand for food, water, and settlement areas, driving the expansion of agricultural lands and urbanization. The establishment of dense road networks and access to water sources for irrigation further facilitate agricultural expansion within the basin.

The fertility of the soils in the basin also plays a significant role in driving LULC change, with different soil types supporting various agricultural activities. It has also propelled the progressive expansion of agricultural and other economic activities within the basin. Ferralitic soils in the southern part of the basin are suitable for plantations and commercial vegetable production, while ferruginous soils in the central and northern parts support crops like cotton, peanut, sorghum, millet, and tobacco. Additionally, the lower zones prone to ponding during rainfall, known as the 'Bas-Fonds' are utilized for rice production [36].

Considering the projected continued population growth in Benin and Africa as a whole, as indicated by the IPCC sixth report, it is imperative to manage land use and land cover change effectively to ensure the sustainability of the environment and inherent resources for current and future generations. This underscores the importance of implementing sustainable land management practices to mitigate the adverse impacts of land use and land cover change on ecosystem and human well-being.

Conclusions

Assessing changes in land use and land cover is crucial for understanding environment dynamics, especially as the 2030 target for the Sustainable Development Goals approaches. This study utilized the Google Earth Engine cloud-based remote sensing tool to analyze land use and land cover changes in the Ouémé River Basin from the year 1986 to 2023. It also examined the Simple Composite Landsat and Random Forest Classifier algorithms in land use and land cover classification. The main findings are as follows:

- In 1986, the basin was predominantly covered by savanna vegetation (69.7 %), with smaller areas of agricultural land (23.3 %), forest areas (6.3 %), settlements and bare lands (0.6 %), and water bodies (0.1 %). However, by 2023, agricultural lands have become the dominant land cover type (51.3 %), with significant decreases in savanna (45.7 %) and forest areas (1.4 %).
- The accuracy assessment revealed that the Simple Composite Landsat and Random Forest algorithms performed well, with overall accuracy values exceeding 90 % and kappa values surpassing 85 %. This indicates the effectiveness of the algorithms in mapping land use and land cover in large and complex ecosystems. Additionally, the Google Earth Engine platform showed promise for robust and reliable mapping of land use and land cover in tropical areas.
- The changes observed in land use and land cover primarily involved the conversions of naturally vegetated areas into agricultural and settlement areas. The annual rates of transformation and fragmentation of LULC increased over the study period, with the highest rates observed from 2015 to 2023 (−4.0 %, 3.0 %, −1.1 %, and 2.2 % for forest areas, settlements/bare lands, savanna areas, and agricultural lands, respectively).

These findings reflect the population growth and urbanization trends in Benin, where demand for food and shelter drives intensive agricultural expansion, leading to deforestation and land degradation. Such changes in the natural ecosystem can impact processes like weather patterns, the hydrological cycle and carbon sequestration. Understanding these impacts on ecosystem functioning and services is essential for promoting sustainable ecosystem management within the basin and therefore recommended for further studies.

CRediT authorship contribution statement

Ernestina Annan: Conceptualization, Formal analysis, Methodology, Writing – original draft, Writing – review & editing, Visualization, Software. **William Amponsah:** Supervision, Writing – review & editing. **Kwaku Amaning Adjei:** Supervision, Writing – review & editing, Methodology. **Markus Disse:** Conceptualization, Supervision, Writing – review & editing. **Jean Hounkpè:** Resources. **Ernest Biney:** Formal analysis, Writing – review & editing. **Albert Elikplim Agbenorhevi:** Writing – review & editing. **Wilson Agyei Agyare:** Supervision, Writing – review & editing, Conceptualization.

Declaration of competing interest

The authors declare that they have no known competing financial interests or personal relationships that could have appeared to influence the work reported in this paper.

Acknowledgments

This research was undertaken under the West African Science Service Center on Climate Change and Adapted Land Use (WASCAL)

programme, funded by the German Federal Ministry of Education and Research (BMBF) at the Kwame Nkrumah University of Science and Technology, Kumasi, Ghana.

Supplementary materials

Supplementary material associated with this article can be found, in the online version, at doi:10.1016/j.sciaf.2024.e02262.

References

[1] O.O. Olofintoye, A.M. Ayanshola, A.W. Salami, A. Idrissiou, J.O. Iji, O.O. Adeleke, A study on the applicability of a SWAT model in predicting the water yield and water balance of the upper Ouémé Catchment in the Republic, Slovak J. Civ. Eng. 30 (1) (2022) 57–66, https://doi.org/10.2478/sjce-2022-0007.

[2] J. Liang, C. Chen, Y. Song, W. Sun, G. Yang, Long-term mapping of land use and land cover changes using Landsat images on the google earth engine cloud platform in Bay area—A case study of Hangzhou Bay, China, Sustainable Horizons 7 (2023) 100061, https://doi.org/10.1016/j.horiz.2023.100061, 2023.

[3] C. Chen, J. Liang, G. Yang, W. Sun, Spatio-temporal distribution of harmful algal blooms and their correlations with marine hydrological elements in Offshore Areas, China, Ocean Coast. Manag. 238 (2023) 106554.

[4] T. Govender, T. Dube, C. Shoko, Remote sensing of land use-land cover change and climate variability on hydrological processes in Sub-Saharan Africa: key scientific strides and challenges, Geocarto Int. 0 (0) (2022) 1–25, https://doi.org/10.1080/10106049.2022.2043451.

[5] The World Bank (2022). *Agricultura, forestry, and fishing, value added (5 of GDP)—Benin. World Bank national accounts data, and OECD National Accounts data files*. https://data.worldbank.org/indicator/nv.agr.totl.zs?locations=BJ.

[6] Q.F. Togbévi, A.Y. Bossa, Y. Yira, K. Preko, A multi-model approach for analysing water balance and water-related ecosystem services in the Ouriyori catchment (Benin), Hydrol. Sci. J. 65 (14) (2020) 2453–2465, https://doi.org/10.1080/02626667.2020.1811286.

[7] The World Bank (2018). *Benin: Broader Access to Water for Rural Communities.* https://www.worldbank.org/en/about/partners/brief/benin-broader-access-to-water-for-rural-communities.

[8] United Nations Environment Programme. (2021). *Progress on Integrated Water Resources Management. Tracking SDG 6 series: global indicator 6.5.1 updates and acceleration needs*. www.un.org/Depts/Cartographic/english/htmain.htm.

[9] A.A. Osseni, H.O. Dossou-Yovo, G.H.F. Gbesso, T.O. Lougbegnon, B. Sinsin, Spatial dynamics and predictive analysis of vegetation cover in the Ouémé River delta in Benin (West Africa), Remote Sens. 14 (2022) 6165, https://doi.org/10.3390/rs14236165.

[10] J. Obodai, K.A. Adjei, S.N. Odai, M. Lumor, Land use/land cover dynamics using Landsat data in a gold mining basin-the Ankobra, Ghana, Remote Sen. Appl. 13 (2019) 247–256, https://doi.org/10.1016/j.rsase.2018.10.007.

[11] C. Hiepe, Soil Degradation by Water Erosion in a Sub-humid West-African Catchment: a Modelling Approach Considering Land Use and Climate Change in Benin, Universität Bonn, Bonn, 2008.

[12] E.I. Biao, Assessing the impacts of climate change on river discharge dynamics in Ouémé River Basin (Benin, West Africa), Hydrology 4 (4) (2017), https://doi.org/10.3390/hydrology4040047.

[13] Y.A. Bossa, Multi-Scale Modeling of Sediment and Nutrient Flow Dynamics in the Ouémé Catchment (Benin)—Towards an Assessment of Global Change Effects on Soil Degradation and Water Quality, Universitäts-und Landesbibliothek, Bonn, 2012.

[14] R. Bodjrènou, F. Comandan, D.K. Danso, Assessment of current and future land use and land cover in the Ouémé basin for hydrological studies, Sustainability (Switzerland) 15 (3) (2023), https://doi.org/10.3390/su15032245.

[15] J. Hounkpè, D.F. Badou, D.M.M. Ahouansou, E. Totin, L.O.C. Sintondji, Assessing observed and projected flood vulnerability under climate change using multi-modeling statistical approaches in the Ouémé River Basin, Benin (West Africa), Reg. Environ. Change 22 (4) (2022) 112, https://doi.org/10.1007/s10113-022-01957-5.

[16] M.C. Peel, B.L. Finlayson, T.A. McMahon, Updated world map of the Köppen-Geiger climate classification, Hydrol. Earth. Syst. Sci. 11 (2007) 1633–1644, https://doi.org/10.5194/hess-11-1633-2007.

[17] A.Y. Bossa, B. Diekkrüger, E.K. Agbossou, Scenario-based impacts of land use and climate change on land and water degradation from the Meso to regional scale, Water (Switzerland) 6 (10) (2014) 3152–3181, https://doi.org/10.3390/w6103152.

[18] T. Noi Phan, V. Kuch, L.W. Lehnert, Land cover classification using google earth engine and random forest classifier-the role of image composition, Remote Sens. (Basel) 12 (15) (2020) 2411, https://doi.org/10.3390/RS12152411.

[19] A. Tassi, M. Vizzari, Object-oriented LULC classification in google earth engine combining SNIC, GLCM, and machine learning algorithms, Remote Sens. 12 (22) (2020) 1–17, https://doi.org/10.3390/rs12223776.

[20] G. Chander, B.L. Markham, D.L. Helder, Summary of current radiometric calibration coefficients for Landsat MSS, TM, ETM+ and EO-1 ALI sensors, Remote Sens. Environ. 113 (2009) 893–903.

[21] US Geological Survey, (2019). *Landsat 8 (L8) Data Users Handbook*, Version 5.0.

[22] S. Qiu, Z. Zhu, P. Olofsson, C.E. Woodcock, S. Jin, Evaluation of Landsat image compositing algorithms, Remote Sens. Environ. 285 (2023) 113375, https://doi.org/10.1016/j.rse.2022.113375.

[23] S. Xie, L. Liu, X. Zhang, J. Yang, X. Chen, Y. Gao, Automatic land-cover mapping using Landsat time-series data based on google earth engine, Remote Sens. 11 (24) (2019), https://doi.org/10.3390/rs11243023.

[24] P. Olofsson, G.M. Foody, M. Herold, S.V. Stehman, C.E. Woodcock, M.A. Wulder, Good practices for estimating area and assessing accuracy of land change, Remote Sens. Environ. 148 (2014) 42–57, https://doi.org/10.1016/J.RSE.2014.02.015.

[25] C. Polykretis, M.G. Grillakis, D.D. Alexakis, Exploring the impact of various spectral indices on land cover change detection using change vector analysis: a case study of Crete Island, Greece, Remote Sens. 12 (2) (2020) 319, https://doi.org/10.3390/rs12020319.

[26] A. Di Gregorio, F. Mushtaq, E. Tchana, M. Aw, R. D'Annunzio, D. Muchoney, B. Mamane, M. Mahamane, B.T. Assoumana, M. Mimouni, E. Aubee, G. O. Enaruvbe, F. Mensah, P. Bartel, M Henry, West African Land Cover Reference System, FAO, AGRHYMET, ECOWAS and OSS., Rome, 2022, https://doi.org/10.4060/cc0730en.

[27] T. Hengle, G.B.M. Heuvelink, B. Kempen, J.G.B. Leenaars, M.G. Walsh, K.D. Shepherd, Mapping soil properties of Africa at 250 m resolution: random forests significantly improve current predictions, PLoS. One 10 (6) (2015) e0125814.

[28] D. García-Álvarez, M. Teresa Camacho Olmedo, M. Paegelow, J. François Mas, Validation Practices with QGIS Land Use Cover Datasets and Validation Tools, 11, Springer Nature Switzerland AG, Gewebestrasse, Cham, Switzerland, 2022, p. 6330, https://doi.org/10.1007/978-3-030-90998-7.

[29] R.G. Pontius, M. Millones, Death to kappa: birth of quantity disagreement and allocation disagreement for accuracy assessment, Int. J. Remote Sens. 32 (15) (2011) 4407–4429, https://doi.org/10.1080/01431161.2011.552923.

[30] Q.F. Togbévi, L.O. Sintondji, Hydrological response to land use and land cover changes in a tropical West African catchment (Couffo, Benin), AIMS. Geosci. 7 (3) (2021) 338–354.

[31] J.R.B. Fisher, E.A. Acosta, P.J. Dennedy-Frank, T. Kroeger, T.M. Boucher, Impact of satellite imagery spatial resolution on land use classification accuracy and modeled water quality, Remote Sens. Ecol. Conserv. 4 (2) (2018) 137–149, https://doi.org/10.1002/rse2.61.

[32] R. Momeni, P. Aplin, D.S. Boyd, Mapping complex urban land cover from spaceborne imagery: the influence of spatial resolution, spectral band set and classification approach, Remote Sens. 8 (2) (2016), https://doi.org/10.3390/rs8020088.

[33] L.M. McNicol, C.M. Ryan, E.T.A. Mitchard, Carbon losses from deforestation and widespread degradation offset by extensive growth in African Woodlands, Nat. Commun. 9 (2018) 3045, 2018, https://www.nature.com/articles/s41467-018-05386-z.pdf.
[34] J.F. Dossou, X.X. Li, N.K. Kouhoundji, E.W. Vissin, Impact of agriculture on the Ouémé basin in Benin, Water. Air. Soil. Pollut. 232 (12) (2021) 1–21, https://doi.org/10.1007/s11270-021-05397-5.
[35] J. Hounkpè, B. Diekkrüger, A.A. Afouda, L.O.C. Sintondji, Land use change increases flood hazard: a multi-modelling approach to assess change in flood characteristics driven by socio-economic land use change scenarios, Nat. Hazards 98 (3) (2019) 1021–1050, https://doi.org/10.1007/s11069-018-3557-8.
[36] Sinsin, B., & Kampmann, D. (eds.) (2010). *Biodiversity Atlas of West Africa, Volume I*: Benin. Cotonou & Frankfurt/Main.